First publ. in: International Journal of Computer Science in Sport (IACSS) ; 10 (2011), 2. - pp. 18-36

Calibration of a Power-Speed-Model for Road Cycling Using Real Power and Height Data

Thorsten Dahmen & Dietmar Saupe

University of Konstanz

Abstract

The relationship between the pedaling power and the speed with road cycling can be described in the form of a dynamical system, that accounts for the inertia and several kinds of mechanical friction. Six out of twelve involved constant parameters are known or can be measured, whereas the determination of the remaining six parameters is prohibitive and depends on the specific cyclist, the bicycle, and the road surface. The sought six parameters occur in the model in only four terms with distinct dependency on power and speed. The parameters are combined to yield one coefficient per term. Using real power and speed measurements on a calibration track and a least squares fitting technique, we estimate these four coefficients. Although the interpretation of the distinct physical phenomena cannot be preserved completely, an experimental evaluation shows that our calibration improves the model speed estimation on both the calibration track and on other tracks with the same type of road surface. Moreover, we compare the significance of the parameters and show that, given precise measurements of a moderately varying slope, the calibration is accurate.

KEYWORDS: ROAD CYCLING, MATHEMATICAL MODEL, PARAMETER CALIBRATION

Introduction

As part of the Powerbike Project at the University of Konstanz, we design methods for data acquisition, modeling, analysis, optimization, and visualization of performance parameters in endurance sports with particular emphasis on competitive cycling (Dahmen, Byshko, Saupe, Röder, & Mantler, 2011). For accurate data acquisition in a laboratory environment, we developed a simulator system that provides a realistic cycling experience on real-world tracks and apply techniques of data processing and training control both online and offline.

The system is based on a Cyclus2 ergometer (RBM Elektronik-Automation GmbH, Leipzig, Germany) that allows to mount arbitrary bicycle frames to its elastic suspension. The eddy current brake, the force of which we control at a sampling rate of 2 Hz, guarantees non-slipping transmission of a braking resistance up to 3000 W. During a ride on the simulator, the applied brake force is computed in real-time as a function of various mechanical friction parameters, the current velocity, and the slope at the current position. A geo-referenced video of the cycling track is synchronized with the current position and the instantaneous performance parameters are monitored. The cyclist operates electronic push buttons on the handlebar to select gears which are simulated by an appropriate resistance control.

One of the major challenges regarding the analysis of performance data and the control of the ergometer brake of the simulator is to define a precise mathematical P-v-model, that describes

the relationship between the pedaling power P and the cycling speed v.

The model reduces the cyclist-bicycle system to a point mass moving forward along a one-dimensional path that is defined by its height as a function of distance. I.e., only forces that contribute to a torque in the crank are considered to have an effect on the cycling speed. Moreover, only the velocity component in the direction of the track, which we refer to as the speed v, is considered.

The model arises from an equilibrium of the propulsion that results from pedaling and resistance components including gravity, inertia, aerodynamic drag, mechanical rolling friction, and friction in the chain and in the bearings. An overview on the relationship between cycling power and speed, in particular aerodynamics and rolling resistance can be found in chapters 4–6 of Wilson, Papadopoulos, and Whitt (2004).

If the slope of a track and the masses of a cyclist and a bicycle are known, basic mechanical laws define the models for gravity and inertia very well. However, the aerodynamic and frictional resistance components rely on complex physical processes that involve a large number of parameters, which are individual and difficult to measure. Hence, simplifications of these processes are inevitable and the determination of the parameters can only be done empirically.

Existing techniques for the estimation of these model parameters can be divided into three categories: laboratory experiments, numerical simulations, and on-road experiments. In the following, we give references to the most prominent and state-of-the-art work related to the empirical determination of the resistance parameters.

As part of extensive research in the area of aerodynamics in sport (Nørstrud, 2008) most effort has been put into the determination of the aerodynamic friction parameters since on level ground and at high speed, aerodynamics clearly contribute the major part to the overall resistance and are very sensitive to the position of the cyclist, clothing, and the bicycle design (Lukes, 2005).

The most accurate parameters are derived from laboratory experiments, i.e., from wind tunnel tests. Reference values for aerodynamic drag parameters with high sensitivity to various positions and cycling equipment are given by García-López et al. (2008) and have been used to optimize the cyclist's position on the bicycle.

Recently, methods of computational fluid dynamics (CFD) have been validated using both drag and surface pressure measurements and were found to provide a better understanding of the flow field information and the origin of the drag force variations than wind tunnel experiments (Defraeye, Blocken, Koninckx, Hespel & Carmeliet, 2010a). A comparison of different CFD techniques applied to a scale model of a cyclist in a wind tunnel yielded that the steady Reynolds-averaged Navier-Stokes shear-stress transport k-ω model and low-Reynolds number modeling for the boundary layer provide the best results concerning three-component forces, moments, and surface pressure (Defraeye, Blocken, Koninckx, Hespel, & Carmeliet, 2010b). It is expected that this conclusion can be generalized to other high-speed applications of bluff-body shapes which arise in disciplines like swimming, skiing, or bob-sleighing, where related CFD techniques have been employed. Simulation results with higher spatial resolutions of individual body segments were presented by Defraeye, Blocken, Koninckx, Hespel, and Carmeliet (2011).

Tire drum testers and computer-controlled drive-train-testing systems, that measure torque and frictional heat using infrared sensors under various conditions, provide the means to examine

rolling resistance and transmission efficiencies in the laboratory (Lafford, 2000; Kyle & Berto 2001; Spicer, Richardson, Ehrlich, & Bernstein, 2000).

However, the technical complexities of these methods are impractical when the assessment of resistance parameters that match a specific cyclist, bicycle, and road surface is required and a mere transfer of established values from the literature is vague because the specific conditions can hardly be controlled or measured precisely. For this reason, on-road techniques were introduced.

Before portable power meters became available, the resistance was either directly measured while towing a cyclists over a flat road behind a motorcycle (di Prampero, Cortili, Mognoni, & Saibene, 1979; Capelli et al., 1993) or performing deceleration measurements (Candau et al., 1999) after which the data have to be fit to the model. Davies (1980) estimated pedaling power in the field assuming that it is equal to the power on an ergometer that causes the same metabolic costs which, however, introduced the physiological variability as an additional source of inaccuracy.

Recent studies have shown that rear-hub or crank-mounted power meters are sensitive enough to quantify the drafting effect (Edwards & Byrnes, 2007) and even measure the resistance parameters for rolling friction and aerodynamic drag when varying body position and tire pressure (Lim et al., 2011). For this purpose a cyclist rides on a smooth asphalt road of 200 m length several times with different but constant velocities in both directions. For each ride one obtains a data point that consists of the squared average velocity and the average resistance force. Then, the coefficients for aerodynamic drag respectively rolling resistance are computed from the slope respectively the intercept of a linear regression line of these data points.

Clearly, their protocol is limited by the ability of the riders to keep a constant speed and the availability of a long flat track that has the desired surface. Therefore, the experiments were performed on a road close to an airport and it was verified that the average power was the same for two rides with equal velocities but opposite directions. In addition, they used surveying equipment and found the roll of the road being less than 0.03% (It was confirmed by the authors that the corresponding inclination angle given in that paper was misprinted.)

In this contribution, we extend their approach in order to overcome the limitations mentioned above by measuring the slope of the track with a differential GPS device and fitting the whole dynamic P-v-model instead of the drag and rolling friction parameters only to the measured power and velocities as varying functions of the distance. Our view on the model is holistic in the sense that we focus on the accuracy of the P-v-relation rather than interpreting our results with respect to the underlying physical phenomena.

Thus, we present an accurate calibration method for the P-v-model that requires only knowledge of the slope profile and measurements of the pedaling power and the speed during rides with a road bicycle on a calibration track. The track may have a moderately varying slope and the cyclists is not required to keep a constant velocity. Furthermore, we perform a sensitivity analysis that reveals which parameters can be estimated accurately.

Our extension has an accuracy requirement regarding the slope of the track that is not provided by the current generation of gps-enabled bicycle computers. But we believe that due to the rapid advancement of navigation systems, in particular the development of the Galileo GNSS, our approach will become applicable without excessive technical equipment in future and hence could be the most accurate and feasible means to determine individual resistance parameters in cycling.

The following section introduces the P-v-model as adopted from (Martin et al., 1998). Subsequently, we present the calibration method and give details of the experimental setup for the rides before the results of the calibration are shown. Thereafter, a sensitivity analysis is performed in order to assess the robustness of our approach.

The Power-Speed-Model

Since the 1980s, mathematical models have been developed to describe the relationship between the pedaling power P and the cycling speed v. These models comprise a multitude of physical phenomena, but only since the advent of rear hub and crank-mounted power meters has it been possible to validate them as done by Martin et al. (1998). They compared outdoor power measurements of the SRM system on a flat road with different constant velocities to power predictions derived from the model, which accounted for over 97 % of the variation of cycling power.

The model equation can be derived from an equilibrium of forces, including the propulsive force F_p, the chain resistance force F_c, the inertial force F_i, the gravity force F_g, the rolling resistance force F_r, frictional resistance forces in the bearings F_b, and the air resistance force F_a:

$$\underbrace{\frac{P}{v}}_{F_p} - \underbrace{\frac{\zeta P}{v}}_{F_c} - \underbrace{\left(m + \frac{I}{r^2}\right)\dot{v}}_{F_i} - \underbrace{mgh'(x)}_{F_g} - \underbrace{mg\mu}_{F_r} - \underbrace{(\beta_0 + \beta_1 v)}_{F_b} - \underbrace{\frac{1}{2}c_d \rho A v^2}_{F_a} = 0\,, \tag{1}$$

subject to

$$x(t)|_{t=0} = 0 \text{ and } v(t)|_{t=0} = v_0\,. \tag{2}$$

The variables v, x, and t are speed, distance, and time, respectively. The other symbols denote parameters and are listed in Table 1.

Known or measurable constants			Specific, not easily measurable constants		
gravity constant	g	9.81 ms^2	chain friction	ζ	2.5 %
air density	ρ	1.2 kgm^3	rolling friction	μ	0.004
mass (cyclist + bike)	m	86.7 kg	bearing friction	β_0	0.091 N
inertia of	I	measured	bearing friction	β_1	0.0087 Nsm
wheels/crank/chain			shape coefficient	c_d	0.7
radius of the wheels	r	335.0 mm	frontal area	A	0.4 m^2
initial speed	v_0	measured	(cyclist and bike)		
Measurable functions of distance					
height profile	$h(x)$	measured			
pedaling power	$P(x)$	measured			

Table 1. Parameters of the P-v-model. Left column: Known or measurable constants and functions of the distance. Right column: The six sought coefficients ζ, μ, β_0, β_1, c_d, and A and literature values adopted from Martin et al. (1998).

We obtain an initial value problem, which has a unique differentiable solution $v(t)$ as output for any input pedaling power P that is a bounded, non-negative, and piecewise continuous

function of time[1]. For real data, a numerical solution can be found with the Runge-Kutta algorithm. In this paper, we use the ode45 function of Matlab.

We eliminate the time, which is irrelevant for our purposes, by dividing (1) by the speed $v = \dot{x}$ and obtain an ordinary differential equation for the speed v as a function of distance x:

$$\frac{P}{v^2} - \frac{\zeta P}{v^2} - \left(m + \frac{I}{r^2}\right) v'(x) - \frac{mgh'(x)}{v} - \frac{mg\mu + \beta_0}{v} - \beta_1 - \frac{1}{2} c_d \rho A v = 0\,, \tag{3}$$

subject to

$$v(x)|_{x=0} = v_0\,. \tag{4}$$

Besides the speed $v(x)$, the pedaling power $P(x)$, and the slope profile of the track $h'(x)$, the model contains 12 physical parameters, as listed in Table 1, which can be assumed to be constant. The values for g and ρ are well known physical constants. The mass of the cyclist and the bicycle m can be weighed with scales. The moment of inertia I of the wheels, the crank, and the chain is estimated experimentally as described in the appendix. The radius of the wheels r is defined by the size of the tires (700×25C corresponds to $r = 2105 \quad \pi \approx$ 335.0 mm). The initial speed v_0 can be measured with a bicycle computer (Garmin Edge 705). The height profile $h(x)$ is measured using a differential GPS device and the power $P(x)$ with an SRM Power Meter as described in the following section.

The remaining six parameters ζ, μ, β_0, β_1, c_d, and A, as given in the right half of Table 1, are constant, but they are difficult to estimate and, in addition, they are specific for the cyclist, the bicycle, or the track.

Parameter Calibration of the P-v-Model

The essential goal of this work is to determine an accurate P-v-model for realistic road cycling. Our approach is to take measurements of height profiles of specific cycling tracks and examine, to what extent the six unknown parameters can be determined by the measured speed and power data on these tracks.

Calibration Method

In the model equation (3), the six sought parameters occur in four terms, which differ in their dependency of the pedaling power P and the speed v. Therefore, only four compound coefficients can be estimated based on power and speed measurements. For notational convenience, we stack the four coefficients into the symbolic parameter vector $\boldsymbol{k}$ and the known or measurable constant parameters into a vector $\boldsymbol{\ell}$:

$$\boldsymbol{k} = \begin{pmatrix} k_1 \\ k_2 \\ k_3 \\ k_4 \end{pmatrix} = \begin{pmatrix} \zeta \\ mg\mu + \beta_0 \\ \beta_1 \\ \frac{1}{2} c_d \rho A \end{pmatrix} \text{ and } \boldsymbol{\ell} = \begin{pmatrix} \ell_1 \\ \ell_2 \\ \ell_3 \\ \ell_4 \end{pmatrix} = \begin{pmatrix} g \\ m \\ v_0 \\ \frac{I}{r^2} \end{pmatrix}. \tag{5}$$

We rewrite the model equation in terms of $\boldsymbol{k}$ and $\boldsymbol{\ell}$:

[1] We confine ourselves to the physically meaningful case, where $v(t) > 0$, i.e., the model does not cover cycling backwards or standing still.

$$\frac{P}{v^2} - \frac{k_1 P}{v^2} - (\ell_2 + \ell_4)v'(x) - \frac{\ell_1 \ell_2 h'(x)}{v} - \frac{k_2}{v} - k_3 - k_4 v = 0\,, \tag{6}$$

subject to

$$v(x)|_{x=0} - \ell_3 = 0\,. \tag{7}$$

In the following we interpret (6) as an implicit definition of the speed function

$$v\colon [0, L] \to \mathbb{R}_+, \tag{8}$$

$$x \mapsto v\big(x; \boldsymbol{k}, \boldsymbol{\ell}, h'(\cdot), P(\cdot)\big)\,, \tag{9}$$

where L is the length of the track.

Given a set of known or measured parameters $\boldsymbol{\ell}$, functions $h'(\cdot)$, $P(\cdot)$, and speed measurements $v_m(x)$ for a specific ride of a cyclist on the given track, our approach is to seek parameters $\boldsymbol{k}$, so that $v(x; \boldsymbol{k})$ is close to the speed measurement $v_m(x)$. Therefore, we define a cost function

$$J(\boldsymbol{k}) = \frac{1}{L}\int_0^L \big(v\big(x; \boldsymbol{k}, \boldsymbol{\ell}, h'(\cdot), P(\cdot)\big) - v_m(x)\big)^2 \,\mathrm{d}x$$

as the mean squared deviation of the modeled speed from the measurement over the length of the track. Then, we determine the estimated parameter vector $\widehat{\boldsymbol{k}}$ as being the argument of the minimum of $J(\boldsymbol{k})$:

$$\widehat{\boldsymbol{k}} = \arg\min_{\boldsymbol{k}} J\,(\boldsymbol{k})\,. \tag{10}$$

Such optimization problems can be solved numerically by gradient-based methods such as the Matlab function lsqcurvefit. In the next but one section we will derive an implicit, analytic formula for the gradient of J, which is beneficial for a robust and efficient implementation of such an optimization.

Data Acquisition on the Tracks

We acquire the coordinates of a 1048 long asphalt cycling track besides the country road from Röhrnang to Liggeringen in south-west Germany (calibration track) using a differential GPS device (Leica GPS900). The sampling period is 1 s. The differential GPS device is attached to a road bicycle (Radeon RPS 9.0), which we push at walking speed along a lane on the cycling track, while we measure the distance by the rotation of the wheels with a common bicycle computer (Garmin Edge 705).

We use the time stamps of the differential GPS device and the bicycle computer to synchronize the distance and height measurements and obtain a precise height profile, the derivative of which with respect to the distance, $h'(x)$, is given in

Figure 1. We selected an only moderately varying profile on purpose, so that gravity does not predominate the resistance forces over those that involve the parameters to be determined. The differential GPS device indicates a 3D-coordinate quality with an error less than 1.8 cm for every measurement point.

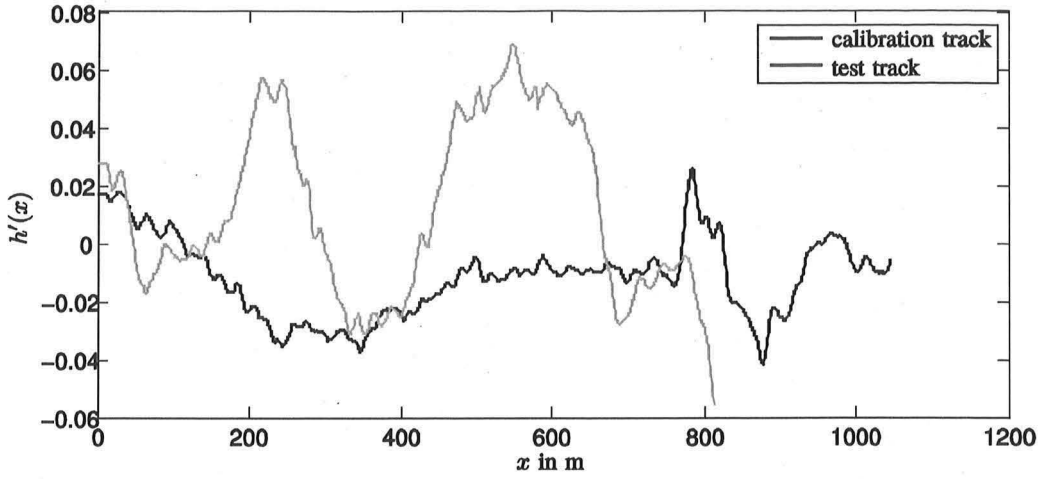

Figure 1. The slopes of the calibration track and the test track.

A cyclist cycles on the road bicycle on the calibration track five times forth and back while there is no wind. The speed is varied in a broad range and the cyclist keeps a constant upright sitting posture. The measured pedaling power $P(x)$, as shown in Figure 2, and the cycling speed $v_m(x)$, Figure 3, are measured by an SRM Power Meter (science edition). This data is used for calibration. The results are presented in the following section.

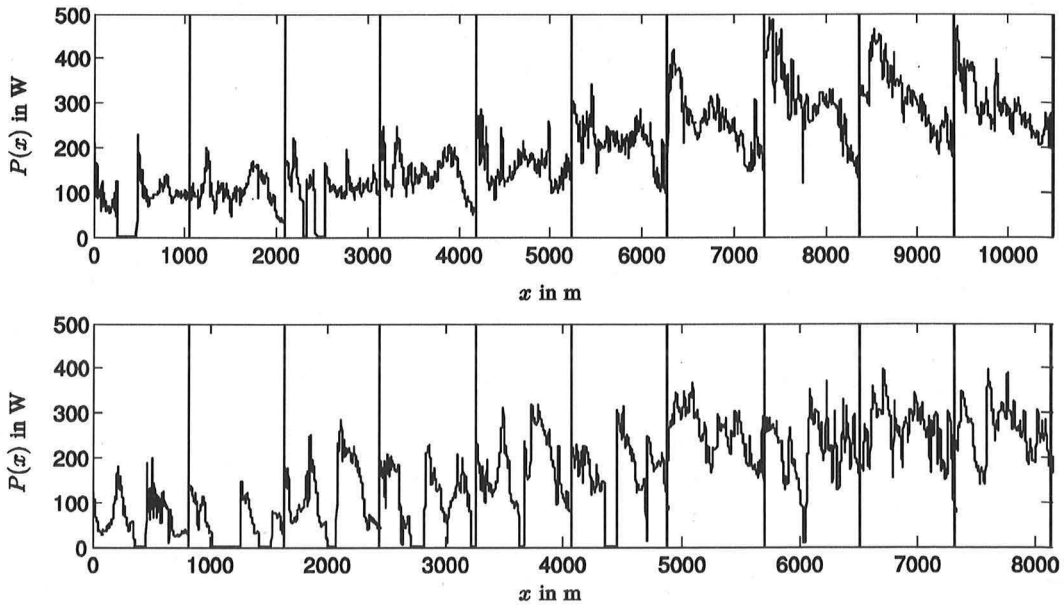

Figure 2. The measured pedaling power $P(x)$ on the calibration track (top) and the test track (bottom). The vertical lines indicate changes of direction at the ends of the track during which the data acquisition was interrupted.

In the same way, measurements are taken on an 813 m long asphalt cycling track in the same area between Allensbach and Kaltbrunn (test track), as depicted in

Figure 1, Figure 2, and Figure 4.

The height profile $h(x)$ is re-sampled on a regular 1 m grid and the smoothed slope $h'(x)$ is obtained using an adaptive-degree polynomial filter (Savitzky-Golay Filter) with a filter length

of 21 m (Barak, 1995).

Calibration Results

In order to demonstrate the results of our calibration approach, we first use the speed and power measurement data of the calibration track to obtain the parameter estimation $\hat{\boldsymbol{k}}$ and compare the speed estimations $v(x;\hat{\boldsymbol{k}})$ of the model to the speed estimation $v(x;\boldsymbol{k}_{lit})$, when using the literature values. For validation, we repeat the comparison on the test track, where we use the same calibrated parameters $\hat{\boldsymbol{k}}$ in order to prove that they can enhance the model accuracy on other than the calibration tracks, too.

Rides on the Calibration Track

Figure 3 shows that the speed estimation of the P-v-model using parameters from literature, $v(x;\boldsymbol{k}_{lit})$, generally exceeds the measured speed $v_m(x)$. The speed estimation using the calibrated parameters $v(x;\hat{\boldsymbol{k}})$ agrees better with the measured speed.

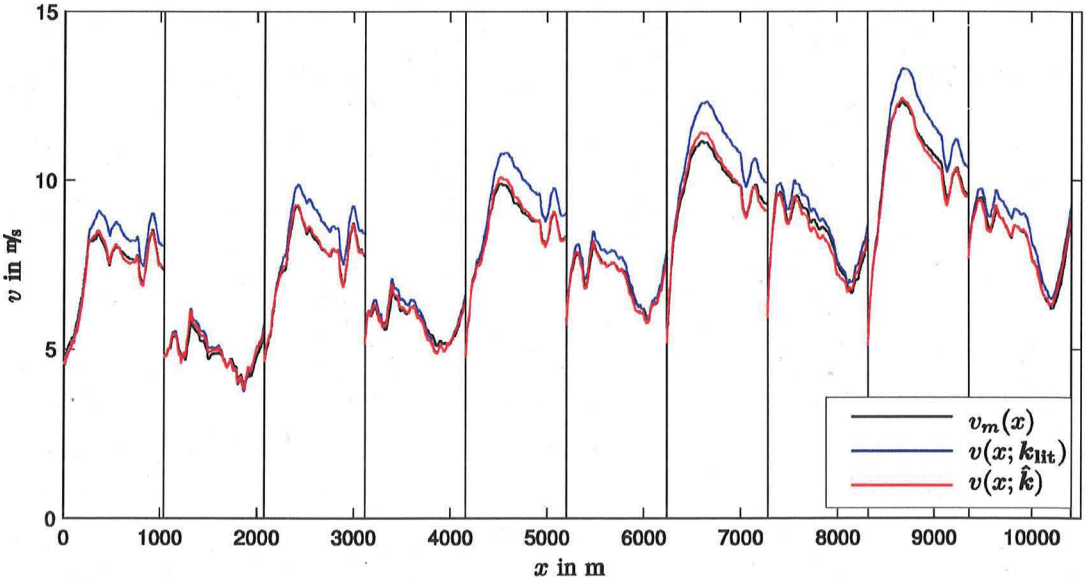

Figure 3. Rides on the calibration track: measured speed $v_m(x)$; speed estimation of the P-v-model, using literature parameters $v(x;\boldsymbol{k}_{lit})$; speed estimation using calibrated parameters $v(x;\hat{\boldsymbol{k}})$.

The numerical values of the literature parameters $\hat{\boldsymbol{k}}_{lit}$ and the calibrated parameters $\hat{\boldsymbol{k}}$ are given in Table 1. We observe that they deviate significantly from the original literature parameters and conclude that the relation to the original physical phenomena is partly lost.

$\boldsymbol{k}$	k_1	k_2	k_3	k_4	$\bar{e}(\boldsymbol{k})$	$\sigma_{e(x;k)}$	$\rho_{v_m(x),v(x;k)}$
$\boldsymbol{k}_{lit}$	2.5 %	3.41 N	0.0087 Nsm	0.168 kgm	0.45 ms	0.35 ms	0.9898
$\hat{\boldsymbol{k}}$	0.3 %	4.22 N	0.076 Nsm	0.257 kgm	0.0073 ms	0.13 ms	0.9943

Table 2. Comparison between numerical values for the parameters $\boldsymbol{k}$ of the P-v-model as taken from literature, $\boldsymbol{k}_{lit}$, and as obtained by calibration, $\hat{\boldsymbol{k}}$; the error function $e(x;\boldsymbol{k}) = v(x;\boldsymbol{k}) - v_m(x)$ is characterized by the mean error $\bar{e}(\boldsymbol{k})$, the standard deviation $\sigma_{e(x;k)}$, and the correlation coefficient $\rho_{v_m(x),v(x;k)}$.

However, the mean error $\bar{e}(\boldsymbol{k}) = \frac{1}{L}\int_0^L e\,(x, \boldsymbol{k})\,\mathrm{d}x$, the standard deviation $\sigma_{e(x;\boldsymbol{k})}$ and the correlation coefficient $\rho_{v_m(x),v(x;\boldsymbol{k})}$ in Table 2 clearly indicate, that the accuracy of the P-v-dynamics has improved. Note, that the residual of the cost function J can be expressed in terms of the mean error $\bar{e}(\boldsymbol{k})$ and the standard deviation $\sigma_{e(x;\boldsymbol{k})}$ as

$$J(\boldsymbol{k}) = \bar{e}^2(\boldsymbol{k}) + \sigma^2_{e(x;\boldsymbol{k})}\,. \tag{11}$$

In the next section, we demonstrate that the impact of the parameters k_1 and k_3 on the speed estimation is very small. Thus, small variations in the estimated speed can result in a considerable change of the parameter estimations $\hat{k}_1$ and $\hat{k}_3$. The parameter estimations $\hat{k}_2$ and $\hat{k}_4$ are more robust. The significant increase in k_4, which is related to the areal resistance coefficients c_d and A contributes the major part to the improvement of the P-v-model accuracy.

Validation Rides on the Test Track

In Lim et al. (2011) the experiments were repeated several times on the same level road in order to obtain empirical standard deviations for the estimated parameters and to show that changes of the experimental conditions have a significant effect on the estimations. As we, in addition, make use of measurements of the slope profile, we validate our method on a different cycling track with a road surface that has similar properties as the calibration track. Using the solution coefficient vector $\hat{\boldsymbol{k}}$, we calculate a model estimation for the speed $v(x;\hat{\boldsymbol{k}})$ of the rides on the test track and compare it to the measured speed as depicted in Figure 4.

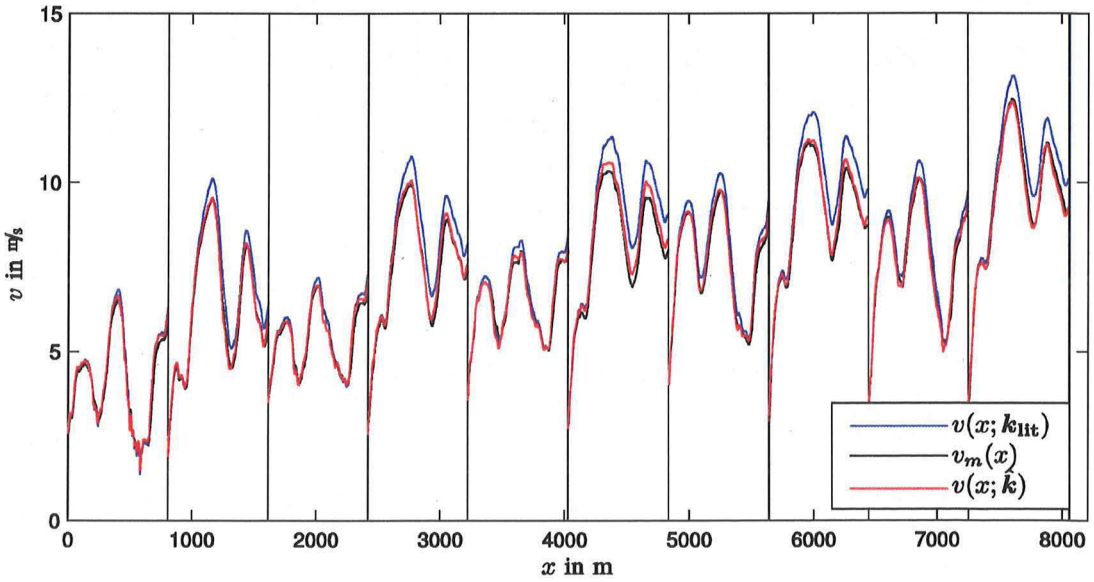

Figure 4. Rides on the test track: measured speed $v_m(\boldsymbol{x})$; speed estimation of the P-v-model, using literature parameters $v(x;\boldsymbol{k}_{lit})$; speed estimation using calibrated parameters $v(x;\hat{\boldsymbol{k}})$.

As indicated by the error measures in Table 3, also on the test track, the match between the measured speed $v_m(x)$ and the speed estimation of the P-v-model $v(x;\boldsymbol{k})$, using the calibrated parameters $\hat{\boldsymbol{k}}$ instead of the literature values $\boldsymbol{k}_{lit}$, is significantly better.

$\boldsymbol{k}$	$\bar{e}(\boldsymbol{k})$	$\sigma_{e(x;\boldsymbol{k})}$	$\rho_{v_m(x),v(x;\boldsymbol{k})}$
$\boldsymbol{k}_{lit}$	0.432 ms	0.350 ms	0.9958
$\widehat{\boldsymbol{k}}$	0.038 ms	0.163 ms	0.9978

Table 3. Error measures for the rides on the test track: absolute mean error of the speed $\bar{e}(\boldsymbol{k})$; standard deviation $\sigma_{e(x;\boldsymbol{k})}$; correlation coefficient $\rho_{v_m(x),v(x;\boldsymbol{k})}$.

The Sensitivity of the Model in Terms of the Parameters in $\boldsymbol{k}$

The influence of the four parameters in $\boldsymbol{k}$ on the model speed estimation is very different. Experience shows that – for a well lubricated chain – the term with the parameter k_1 in (6) is negligible. The terms with the parameters k_2, k_3, and k_4 depend on the speed only. Figure 5 depicts how these coefficients contribute to the total resistance force which is directly proportional to their contribution to the acceleration $\dot{v}(x)$.

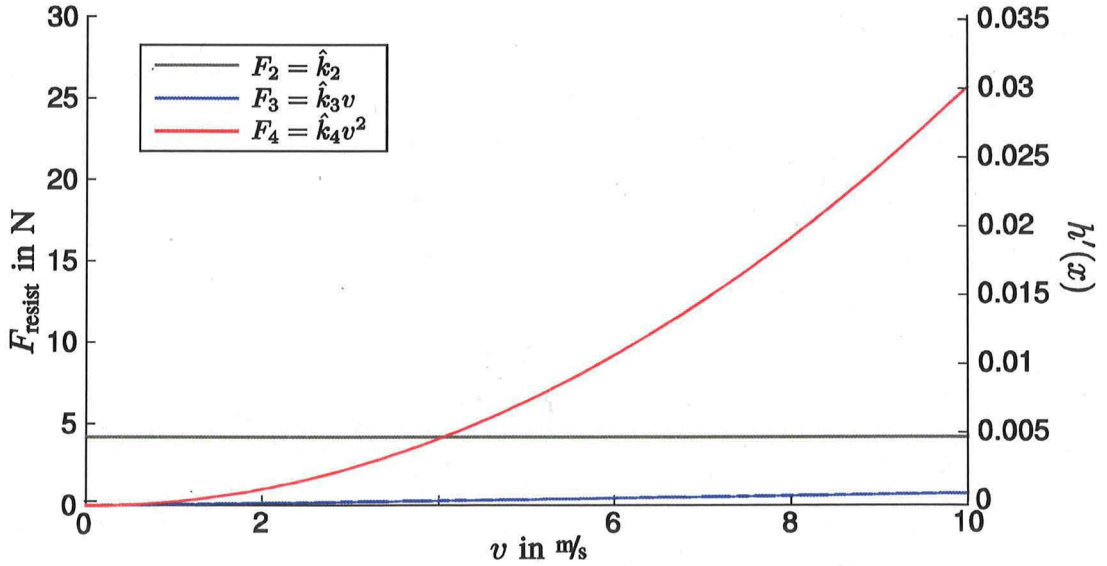

Figure 5. The contributions of the terms with the parameters k_2, k_3, and k_4 on the total resistance force F_{resist}. At $v = 4.05$ ms, the influence of k_4 becomes larger than the influence of k_2. The coefficient k_3 plays a minor role. The right ordinate axis indicates the slope $h'(x)$, that causes an equivalent resistance force.

For $v < 4.05\,ms$ the coefficient k_2 contributes the largest share to the total resistance force whereas for higher velocities, k_4 is dominant. The coefficient k_3 is in fact negligible for all practical purposes.

The right ordinate axis indicates the contribution of the slope $h'(x)$ to the resistance force. Its influence can easily exceed the influence of the other resistance components. Therefore, the slope of the calibration track may vary, but its magnitude should be moderate and it must be measured with high accuracy to ensure a successful parameter calibration. Note that the limitation on the magnitude of the slope only refers to the calibration track. Once the parameters have been determined, the model can be applied to steep tracks, if precise slope data are available for the track. In this situation the gravity component just becomes more influential.

However, these simple considerations are rather static and do not allow us to fully grasp how

changes in the parameters $\boldsymbol{k}$ affect the model output speed $v(x;\boldsymbol{k})$. Therefore, we make use of a local method of sensitivity analysis and compute the partial derivatives of the model estimation output $\frac{\partial v(x;\boldsymbol{k})}{\partial \boldsymbol{k}}$. Eventually, the quantities

$$s_{k_i}(x) = \frac{k_i}{v}\frac{\partial v(x;k_i)}{\partial k_i} \tag{12}$$

quantify the sensitivity of the model output $v(x;k_i)$ with respect to the parameters k_i, since they give the relative change of the model output speed $v(x)$, due to a relative change in the parameters in $\boldsymbol{k}$. In case the effect is small, we conclude, that the minimum $J(\widehat{\boldsymbol{k}})$ cannot be pronounced and hence the calibration method is not robust with respect to the considered parameter.

Besides, the partial derivatives are very beneficial in the implementation of our calibration method, because they are required for the computation of the gradient of our cost function

$$\frac{\partial}{\partial \boldsymbol{k}}\big(J(\boldsymbol{k})\big) = \frac{2}{L}\int_0^L \big(v(x) - v_m(x)\big)\frac{\partial v}{\partial \boldsymbol{k}}\,\mathrm{d}x\,. \tag{13}$$

The result facilitates gradient-based numerical optimization to solve (10).

In order to derive the partial derivatives, we make use of the theorem of implicit functions and define a function $\boldsymbol{f} = (f_1, f_2)^T$ to be equal to the left-hand side of (6):

$$\begin{aligned}&\boldsymbol{f}(v(x;\boldsymbol{k}), v'(x;\boldsymbol{k});\boldsymbol{k},\boldsymbol{\ell}, h'(\cdot), P(\cdot))\\ &= \begin{pmatrix} \dfrac{P}{v^2} - k_1\dfrac{P}{v^2} - (\ell_2+\ell_4)v'(x) - \dfrac{\ell_1\ell_2 h'(x)}{v} - \dfrac{k_2}{v} - k_3 - k_4 v \\ v(x)|_{x=0} - \ell_3 \end{pmatrix}.\end{aligned} \tag{14}$$

Furthermore, let

$$\boldsymbol{F}(\boldsymbol{k}) := \boldsymbol{f}(v(x;\boldsymbol{k}), v'(x;\boldsymbol{k});\boldsymbol{k},\boldsymbol{\ell}, h'(\cdot), P(\cdot)) \quad \forall\, \boldsymbol{k} \in \mathbb{R}^4_+. \tag{15}$$

Then,

$$\boldsymbol{F}(\boldsymbol{k}) \equiv \boldsymbol{0} \quad \forall\, \boldsymbol{k} \in \mathbb{R}^4_+, \tag{16}$$

and all derivatives clearly vanish:

$$\frac{d\boldsymbol{F}}{d\boldsymbol{k}} = \boldsymbol{0}. \tag{17}$$

We apply the chain rule for differentiation and obtain

$$\frac{d\boldsymbol{F}}{d\boldsymbol{k}} = \frac{\partial \boldsymbol{f}}{\partial v}\frac{\partial v}{\partial \boldsymbol{k}} + \frac{\partial \boldsymbol{f}}{\partial v'}\frac{\partial v'}{\partial \boldsymbol{k}} + \frac{\partial \boldsymbol{f}}{\partial \boldsymbol{k}} = 0 \tag{18}$$

The partial derivatives $\frac{\partial \boldsymbol{f}}{\partial v}$, $\frac{\partial \boldsymbol{f}}{\partial v'}$, and $\frac{\partial \boldsymbol{f}}{\partial \boldsymbol{k}}$, can be computed from (14). We obtain four nonlinear, first-order differential equations with four initial values whose solutions are the sought derivatives $\frac{\partial v}{\partial k_i}$:

$$\left(-\frac{2P}{v^3}+\frac{2k_1P}{v^3}+\frac{\ell_1\ell_2}{v^2}h'(x)+\frac{k_2}{v^2}-k_4\right)\frac{\partial v}{\partial k_i}-(\ell_2+\ell_4)\frac{\mathrm{d}}{\mathrm{d}x}\left(\frac{\partial v}{\partial k_i}\right)-\mathcal{K}_i=0 \qquad (19)$$

with

$$\left.\frac{\partial v}{\partial k_i}\right|_{x=0}=0 \quad \text{and} \quad \mathcal{K}_i=\begin{cases}\dfrac{P}{v^2} & \text{for } i=1\\ \dfrac{1}{v} & \text{for } i=2\\ 1 & \text{for } i=3\\ -v & \text{for } i=4\end{cases}. \qquad (20)$$

Again, the solutions can be computed with the Runge-Kutta method.

Figure 6 depicts the relative sensitivities of the model estimation speed $v(x;\widehat{\boldsymbol{k}})$ with respect to the calibration parameters in $\boldsymbol{k}$. All sensitivities are negative, since the parameters characterize resistances.

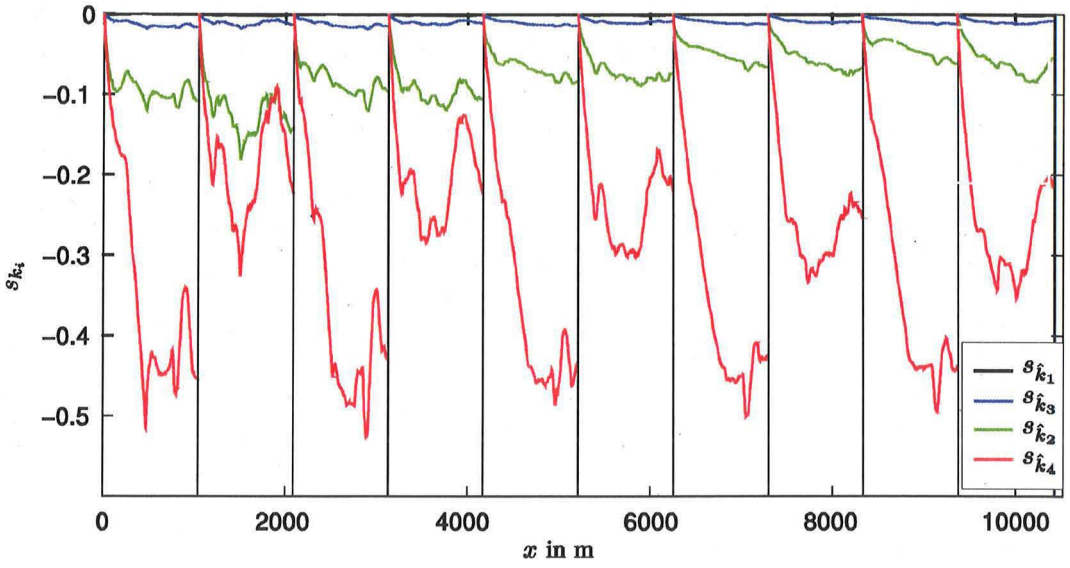

Figure 6. The relative parameter sensitivities s_{k_i}, defined in (12). The sensitivity s_{k_1} is so insignificant, that it almost coincides with the abscissa.

The graph confirms our previous assumption that the influence of the parameters k_1 and k_3 is very small and we conclude that on the one hand, our estimation method cannot be robust, but on the other hand an accurate estimation of the insensitive parameters k_1 and k_3 is not essential for a precise model speed estimation, either.

At the beginning of each ride, the sensitivity of every parameter vanishes, because the initial speed is solely defined by $\ell_3 = v_0$. In the course of each ride, the parameters gain influence. The moment of inertia determines how fast this influence is gained and demands a minimum length of the track for a sensible calibration. In particular with high velocities, k_4 is the most influential parameter and hence, its estimation is the most robust.

The method of computing partial derivatives and sensitivities can be applied in other contexts, as well, e.g., to quantify the influence of the known or measurable parameters $\boldsymbol{\ell}$, as

demonstrated in the appendix.

Limitations

Our calibration method estimates parameters to determine an holistic model that defines the relationship between pedaling power and cycling speed if power and height data are provided. However, there are limitations concerning both the model and the calibration method, which we discuss in this section.

The model itself contains several simplifications. Reducing the cyclist-bicycle system to a point mass neglects that we deal with a multi-segmental unit. The P-v-model does not consider relative movements and internal forces within that unit except of the resulting pedal force. The effects of, e.g., braking or pumping[2] on the cycling speed are omitted.

Furthermore, as only the speed of the point mass along a one-dimensional path is modeled, centripetal forces and gyroscopic effects in curves are discounted.

The holistic approach ensures that conditions like air density, road surface properties, or the shape of the cyclist-bicycle system are implicitly accounted for with respect to their impact on the speed. On the one hand, this is an advantage of our approach. On the other hand it is not possible to compute the compound parameters as functions of individual measurements of these conditions.

The calibration method is limited by the accuracy of the power meter, as discussed in and the differential gps device. In presence of obstacles close to the track like vegetation or settlements, the gps signal quality is degraded. The calibration track may have a moderately varying slope, however, the parameter sensitivity decreases with the magnitude of that slope.

Some of the limitations mentioned above like braking and pumping are less relevant in terms of road cycling time trials, in particular if the primary focus is on optimizing the distribution of the physical performance rather than the skillfulness of a cyclist on a specific track.

Regarding the simulator, additional limitations coincide with limitations of the simulator itself: The simulation speed is defined by the rotation of the ergometer flywheel which can only be accelerated by pedaling and not by braking or pumping at all. Though having an elastic suspension that allows for a sway pedal stroke, steering and centripetal forces are not simulated and the flywheel axis is fixed so that there are no gyroscopic effects. As the ergometer is non-motorized, we focus on cycling tracks without steep descents where braking is less relevant.

For these reasons, we consider our model and calibration method to be appropriate with respect to the available measurement devices and in particular to the application in cycling simulators.

Conclusions

The standard P-v-model has six constant physical parameters, the values of which cannot be easily determined by direct measurements. However, they can be substituted by four symbolic coefficients, which can be estimated given the profile of a track and simultaneous measurements of the pedaling power and the speed on the same track, in order to obtain an accurate P-v-model which is specific for the cyclist, the bicycle, and the road surface.

The calibration method should be carried out on moderately varying calibration tracks and a

[2] Pulling the cyclist's center of mass down and pushing it up again while passing a summit.

precise measurement of the slope profile as, e.g., with a differential GPS device is essential for a successful calibration. Furthermore, the accuracy is obtained at the cost of partly losing the physical interpretation of the parameters.

Yet, we demonstrated, that not only are the calibrated parameters valid on the track on which they have been estimated, but they can also improve the speed estimation on other tracks with the same road surface properties.

In fact, only two out of the four parameters have a significant influence in the P-v-model. The parameter that originates from the aerodynamic drag coefficients is dominant for velocities higher than $4\ ms$.

Outlook

The results of the parameter calibration will be used in future for the control of the braking force of the simulator and for the analysis of outdoor power and speed data for the following purposes.

In spite of the high accuracy of the differential GPS-device, it remains difficult to precisely measure the slope, since the GPS signal quality is disturbed by trees, buildings, or other obstacles on the roadside, so that the differential correction cannot be performed. Therefore, we plan to fuse the height measurements obtained from the differential GPS device with an estimation of the slope that can be computed by resolving the model equation (6) for $h'(x)$. It has been proven in many practical examples, where position data is aided by inertial navigation systems, that the Kalman smoother is the optimal linear estimator for this application.

Furthermore, a computer program is currently being developed, that allows to change any parameter of the P-v-model and visualize the effects on all the other parameters to explore any specific real scenario interactively.

Another major research question within the context of the Powerbike project is the computation of an optimal pacing strategy that assists the athlete to complete a specific course in minimal time. Mathematically, this can be formulated as an optimal control problem, where pedaling power is the control variable to be optimized, time to complete the course is the cost functional, and the P-v-model is the mechanical part of the dynamical system.

In addition, a physiological endurance model, limiting the admissible pedaling power according to the energy reserves of the cyclist, is required. Such whole-body bio-energetic models have been reviewed by Morton (2006).

An analytical treatment of the optimization problem for synthetic and piecewise constant slope profiles, and a simplified mechanical and physiological model has been presented by Gordon (2005). A numerical implementation of this approach, that accounts for varying slopes and mechanical inertia, has been implemented and tested on our simulator (Wolf & Dahmen, 2010). Yet, we believe, that a refinement of the physiological model and the methods for estimating its parameters is necessary, before the system can be used to train strategies in practice.

Therefore, we plan to use lactate measurements and spiroergometry for the calibration of the physiological model and to design real-time feedback and a model predictive control for time trials both on the simulator and in the field. For the optimization of group training in cycling a related model-predictive control uses a model for the cyclist's power demand according to the position within the group and the heart rate as physiological stress indicator (Le, 2010).

All these applications rely on the accuracy of the P-v-model, whereas the physical interpretation of the parameters is less important. Therefore, we consider the parameter calibration as an important basis element that will improve the accuracy of the results in various future applications.

References

Barak, P. (1995). Smoothing and differentiation by an adaptive-degree polynomial filter. *Analytical Chemistry, 67*(17), 2758–2762.

Candau, R. B., Grappe, F., Ménard, M., Barbier, B. Millet, G. Y., Hoffman, M. D., Belli, A.R., & Rouillon, J. D. (1999). Simplified deceleration method for assessment of resistive forces in cycling. *Medicine & Science in Sports & Exercise, 31*(10), 1441–1447.

Capelli C., Rosa G., Butti F., Ferretti G., Veicsteinas A., & Prampero P. E. di. (1993). Energy cost and efficiency of riding aerodynamic bicycles. European Journal of Applied Physiology and Occupational Physiology, *67*(2), 144–149.

Dahmen, T., Byshko, R., Saupe, D., Röder, M., & Mantler, S. (2011). Validation of a model and a simulator for road cycling on real tracks. *Sports Engineering, 2*(14), 95–110.

Dahmen, T. (2010). Kalibrierung eines Leistungs-Geschwindigkeits-Modells für Rennradfahrten mit realen Leistungs- und Höhendaten [Calibration of a performance veolcity model for road cycling based on real performance and altitude data]. In J. Wiemeyer, D. Link, R. Angert, B. Holler, A. Kliem, N. Roznawski, D. Schöberl, & M. Stroß (Eds.), Sportinformatik trifft Sporttechnologie [Sports Informatics meets Sports Technology]. 8. Symposium of the dvs Section Sports Informatics, 15.–17. September, Darmstadt, 235–239.

Davies, C. T. (1980). Effect of air resistance on the metabolic cost and performance of cycling. *European Journal of Applied Physiology and Occupational Physiology, 45*(2), 245–254.

Defraeye T., Blocken B., Koninckx E., Hespel P., & Carmelietd J. (2010a). Aerodynamic study of different cyclist positions: CFD analysis and full-scale wind-tunnel tests. *Journal of Biomechanics, 43*(7), 1262–1268.

Defraeye T., Blocken B., Koninckx E., Hespel P., & Carmelietd J. (2010b). Computational fluid dynamics analysis of cyclist aerodynamics: Performance of different turbulence-modeling and boundary-layer modeling approaches. *Journal of Biomechanics, 43*(12), 2281–2287.

Defraeye T., Blocken B., Koninckx E., Hespel P., & Carmelietd J. (2011). Computational fluid dynamics analysis of drag and convective heat transfer of individual body segments for different cyclist positions. *Journal of Biomechanics, 44*(9), 1695-1701.

Edwards, A. G., & Byrnes, W. C. (2007). Aerodynamic Characteristics as Determinants of the Drafting Effect in Cycling. *Medicine & Science in Sports & Exercise, 39*(1), 170–176.

García-López, J., Rodríguez-Marroyo J. A., Juneau, C.-E., Peleteiro J., Martínez A., & Villa, J. G. (2008). Reference values and improvement of aerodynamic drag in professional cyclists. *Journal of Sports Sciences, 26*(3), 277–286.

Gordon, S. (2005). Optimizing distribution of power during a cycling time trial. *Sports Engineering, 8*(2), 81–90.

Gressmann, M. (2002). Fahrradphysik und Biomechanik. Technik – Formeln – Gesetze [Technique – Formula – Law]. (7. Edition). Delius Klasing Verlag.

Kyle, R., & Berto, F. (2001). The mechanical efficiency of bicycle derailleur and hub-gear transmissions. *Human Power*, 52, 3–11.
Lafford, J. (2000). Rolling resistance of bicycle tires. *Human Power*, *50*, 14–19.
Le, A. (2010). Sensor-based training optimization in professional cycling by model predictive control. Shaker Verlag GmbH, Germany.
Lim, A. C., Homestead, E. P., Edwards, A. G., Carver, T. C., Kram, R., & Byrnes, W. C. (2011). Measuring changes in aerodynamic/rolling resistances by cycle-mounted power meters. *Medicine & Science in Sports & Exercise*, *43*(5), 853–860.
Lukes, R. A., Chin, S. B., Haake, S. J. (2005). The understanding and development of cycling aerodynamics. *Sports Engineering*, *8*(2), 59–74.
Martin, J. C., Milliken, D. L., Cobb, J. E., McFadden, K. L., & Coggan, A. R. (1998). Validation of a mathematical model for road cycling power. *Journal of Applied Biomechanics*, *14*(3), 276–291.
Morton, R. H. (2006). The critical power and related whole-body bio-energetic models. *European Journal of Applied Physiology, 96*(4), 339–354.
Nørstrud H. (Ed.). (2008). *Sport Aerodynamics*. (1st ed.). Springer.
Spicer, J. B., Richardson C. J. K., Ehrlich, M. J. & Bernstein J. R. (2000). On the efficiency of bicycle chain drives. *Human Power*, *50*, 3–9.
Wilson, D. G., Papadopoulos, J., & Whitt, F. R. (2004). *Bicycling Science 3rd Ed.*. The MIT Press, USA.
Wolf, S., & Dahmen, T. (2010). Optimierung der Geschwindigkeitssteuerung bei Zeitfahrten im Radsport [Optimization of velocity control at time trial in road cycling]. In J. Wiemeyer, D. Link, R. Angert, B. Holler, A. Kliem, N. Roznawski, D. Schöberl, & M. Stroß (Eds.), *Sportinformatik trifft Sporttechnologie* [Sports Informatics meets Sports Technology]. 8. Symposium of the dvs Section Sports Informatics,, 15.–17. September, Darmstadt, 235–239.

Appendix

The Accuracy of the Power Meter Devices

In Dahmen (2010), an SRM Power Meter V, professional edition with four strain gauges, was used for which the manufacturer claims an accuracy of ± 2 %. For the experiments in this paper, we used a SRM Power Meter IIV, scientific edition, with 8 strain gauges and an accuracy of 0.5 . However, a perfect reference for pedaling power does not exist and inquiries on the manufacturer's calibration method revealed that the accuracies of power meters have not been evaluated scientifically.

In order to compare the calibrations of our two SRM Power Meters, we perform a step test ranging from $80 - 300$ W on a Cyclus2 ergometer and computed the averages of the SRM power measurements during each step, as depicted in Figure 7.

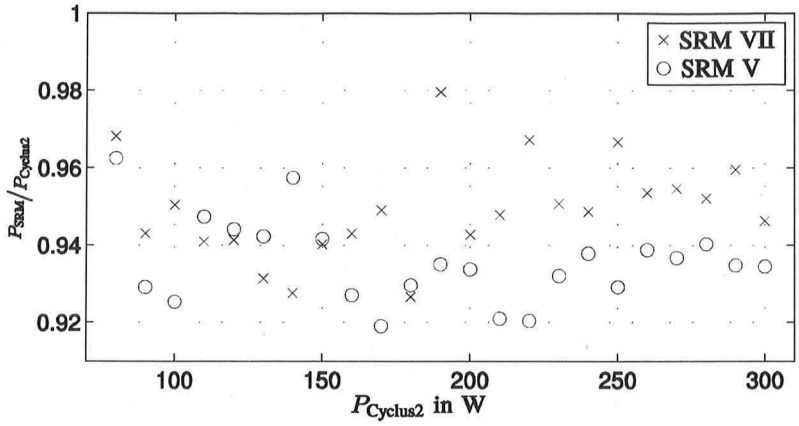

Figure 7. Comparison of power measurements of an SRM Power Meter IIV and an SRM Power Meter V. Both devices were used to measure the power during a step test on a Cyclus2 ergometer (power range: $80 - 300$, step duration 30 s, cadence 80 rpm. The SRM measurement power P_{SRM} divided by the nominal power of the Cyclus2, $P_{Cyclus2}$ for each step is plotted versus $P_{Cyclus2}$. For the Cyclus2 ergometer, the manufacturer claims an accuracy of ± 2 % for $P > 250$ and $\pm 5\ W$ for $P < 250$ W. All devices were either new or recently calibrated by the manufacturer.

In fact, we had expected, that the SRM power meters display a slightly larger power since they measure the sum of the power absorbed by the ergometer brake, the frictional resistance of the ergometer mechanics, and the frictional resistance of the chain and the crank of the bicycle, whereas the nominal power of the ergometer should be equal to the power absorbed by the ergometer brake only. However, we observe that both SRM devices measure significantly less power than the nominal power during each step. Moreover, particularly with a nominal power above 200 W, we detect that the power measurements of the Power Meter VII exceed those of the Power Meter V.

We conclude that the determination of the parameters of the P-v-model with our method is affected by the lack of a reliable calibration method of power meters. Even if model estimations and measurements match well, we have to be aware of a possible additional error regarding the unknown true pedaling power.

Estimation of Wheel, Crank, and Chain Inertia

The moments of inertia of a bicycle wheel can be determined by hanging up the wheel in a horizontal position and having it oscillate around its axis, Gressmann (2002).

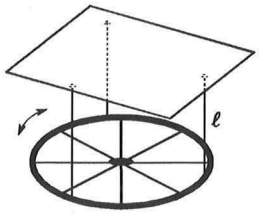

Figure 8. Setup of a pendulum experiment for the determination of the wheel inertia.

For this purpose, we fasten three equally long pieces of string to three equally spaced points on the rim, as sketched in Figure 8. The other ends of the pieces of string are fixed to a horizontal board above the wheel, so that the pieces of string are vertical when the system is at rest. The inertia I_w of this physical pendulum is

$$I_w = \frac{T^2 mg\ell}{4\pi^2}, \tag{21}$$

where T is the oscillation period, ℓ is the length of the pieces of string. With the wheel oscillating, we measure the time for 20 periods and compute a momentum of $I_{wf} = 0.14$ [2] for the front wheel an and $I_{wr} = 0.16\ \mathrm{kgm}^2$ for the rear wheel.

The inertia of the crank is composed of the inertia of the pedals I_p, of the crank arm I_a, of the chainrings I_c, and of the SRM Power Meter I_{SRM}. Each component can be approximated by a primitive geometric form rotating around the center of the crank axis: (pedal – point mass, crank arm – solid cylinder, chainrings – rings, SRM – solid disk).

We measure the weights and the sizes of each component and compute the individual moments of inertia. Their sum yields the total inertia of the crank $I_c = 0.02\ \mathrm{kgm}^2$.When the cyclist does not pedal ($P = 0$), only the wheels and not the crank contribute to the inertia. The resulting moment of inertia I of the wheels, the crank, and the chain is

$$I = \begin{cases} I_{wf} + I_{wr} & \text{for } P = 0 \\ I_{wf} + I_{wr} + \gamma^2 I_c + r_s^2 m_{ch} & \text{for } P > 0, \end{cases} \tag{22}$$

with γ being the transmission ratio, r_s is the radius of the rear sprocket wheel currently used by the chain, and m_{ch} is the mass of the chain.[3] The transmission ratios in the experiments can be reconstructed from the measured cadence f_c:

$$\gamma = \frac{v}{f_c r_w}. \tag{23}$$

The details of these computations for our experiments are omitted since this is straightforward and the inertia only has a negligible impact in the P-v-model.

Sensitivities and Partial Derivatives of the Speed With Respect to ℓ

The sensitivities s_{l_i} of the speed estimation of the model with respect to the parameters in $\boldsymbol{\ell}$ can be derived in analogy to the derivation of the sensitivities s_{k_i}. First, we derive the differential equations for $\frac{\partial v}{\partial \ell_i}$, which correspond to (20):

$$\left(-\frac{2P}{v^3} + \frac{2k_1 P}{v^3} + \frac{\ell_1 \ell_2}{v^2} h'(x) + \frac{k_2}{v^2} - k_4\right)\frac{\partial v}{\partial \ell_i} - (\ell_2 + \ell_4)\frac{d}{dx}\frac{\partial v}{\partial \ell_i} - \mathcal{L}_i = 0, \tag{24}$$

where

$$\left.\frac{\partial v}{\partial \ell_i}\right|_{x=0} = \begin{cases} 0 & \text{for } i = 1,2,4 \\ 1 & \text{for } i = 3 \end{cases} \quad \text{and} \quad \mathcal{L}_i = \begin{cases} \frac{m}{v} h'(x) & \text{for } i = 1 \\ v'(x) + \frac{g}{v} h'(x) & \text{for } i = 2 \\ 0 & \text{for } i = 3 \\ v'(x) & \text{for } i = 4 \end{cases}. \tag{25}$$

Then, we define the sensitivities of the model estimation speed with respect to the parameters in $\boldsymbol{\ell}$ in analogy to (12):

[3] During the rides for the calibration experiments, gear changes were avoided, not to disturb the power measurement.

$$s_{\ell_i}(x) = \frac{\ell_i}{v}\frac{\partial v(x;\ell_i)}{\partial \ell_i}. \tag{26}$$

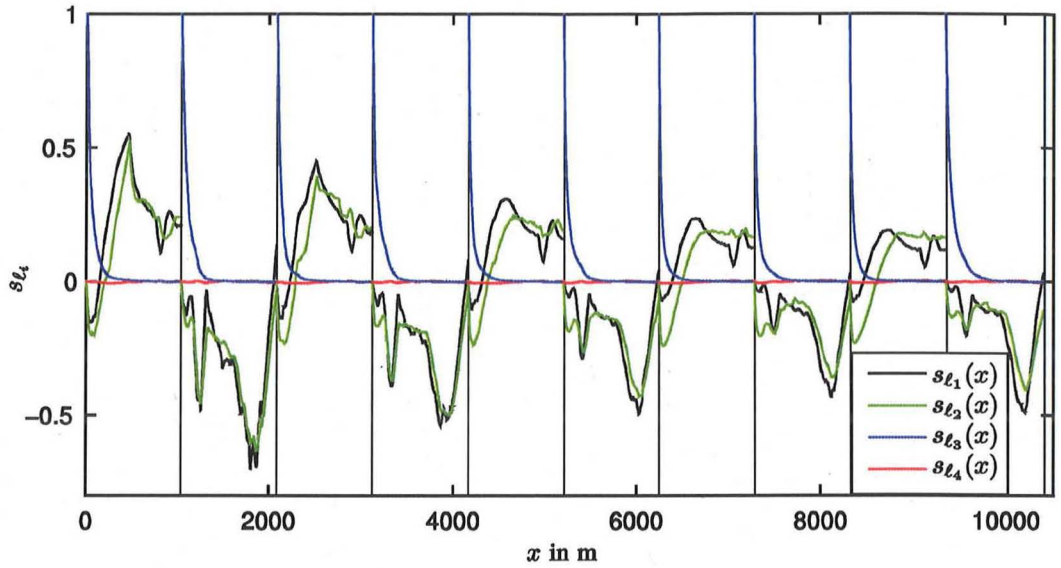

Figure 9. Sensitivities s_i of the model estimation speed $v(x;\widehat{\boldsymbol{k}})$ with respect to the parameters in $\boldsymbol{\ell}$.

Figure 9 depicts the sensitivities s_{ℓ_i} for the rides on the calibration track. At the beginning of each ride, the initial speed ℓ_3 is dominant because for $x = 0$ the speed is solely defined by the initial speed v_0. However, its influence decreases rapidly and after 200 m the sensitivity with respect to the gravity factor $g = \ell_1$ and to the mass $m = \ell_2$ reveal the largest impact on $v(x;\widehat{\boldsymbol{k}})$. The moment of inertia of the wheels, the crank, and the chain, which is represented by ℓ_4 is negligible.

Figure 6 and Figure 9 allow a direct comparison of the sensitivities of all parameters of the P-v-model.